




Diurnally fluctuating $p\text{CO}_2$ enhances growth of a coastal strain of *Emiliana huxleyi* under future-projected ocean acidification conditions

Futian Li ^{1,2,3,†}, Jiekai Xu^{1,†}, John Beardall^{1,4}, and Kunshan Gao^{1,2*}

¹State Key Laboratory of Marine Environmental Science/College of Ocean and Earth Sciences, Department of Marine Biological Science and Technology, Xiamen University, Xiamen 361102, China

²Co-Innovation Center of Jiangsu Marine Bio-industry Technology, Jiangsu Ocean University, Lianyungang 222005, China

³Jiangsu Institute of Marine Resources Development, Lianyungang 222005, China

⁴School of Biological Sciences, Monash University, Clayton, VIC 3800, Australia

*Corresponding author: tel: 86-592-2187982; fax: 86-592-2187963; e-mail: ksgao@xmu.edu.cn.

†These two authors contributed equally to this work.

Li, F., Xu, J., Beardall, J., and Gao, K. Diurnally fluctuating $p\text{CO}_2$ enhances growth of a coastal strain of *Emiliana huxleyi* under future-projected ocean acidification conditions. – ICES Journal of Marine Science, doi:10.1093/icesjms/fsab036.

Received 23 September 2020; revised 8 February 2021; accepted 13 February 2021.

The carbonate chemistry in coastal waters is more variable compared with that of open oceans, both in magnitude and time scale of its fluctuations. However, knowledge of the responses of coastal phytoplankton to dynamic changes in pH/ $p\text{CO}_2$ has been scarcely documented. Hence, we investigated the physiological performance of a coastal isolate of the coccolithophore *Emiliana huxleyi* (PML B92/11) under fluctuating and stable $p\text{CO}_2$ regimes (steady ambient $p\text{CO}_2$, 400 μatm ; steady elevated $p\text{CO}_2$, 1200 μatm ; diurnally fluctuating elevated $p\text{CO}_2$, 600–1800 μatm). Elevated $p\text{CO}_2$ inhibited the calcification rate in both the steady and fluctuating regimes. However, higher specific growth rates and lower ratios of calcification to photosynthesis were detected in the cells grown under diurnally fluctuating elevated $p\text{CO}_2$ conditions. The fluctuating $p\text{CO}_2$ regime alleviated the negative effects of elevated $p\text{CO}_2$ on effective photochemical quantum yield and relative photosynthetic electron transport rate compared with the steady elevated $p\text{CO}_2$ treatment. Our results suggest that growth of *E. huxleyi* could benefit from diel fluctuations of pH/ $p\text{CO}_2$ under future-projected ocean acidification, but its calcification was reduced by the fluctuation and the increased concentration of CO_2 , reflecting a necessity to consider the influences of dynamic pH fluctuations on coastal carbon cycles associated with ocean global changes.

Keywords: calcification, CO_2 , coccolithophore, *Emiliana huxleyi*, fluctuation, ocean acidification, photosynthesis

Introduction

The oceans have absorbed about one-third of the anthropogenically released CO_2 (Sabine *et al.*, 2004), leading to a decrease in seawater pH (0.1 pH units since the preindustrial era) and carbonate ions, along with increases in aqueous CO_2 and bicarbonate, a process known as ocean acidification (OA). The effects of OA on coccolithophores, one of the most important calcifying microalgal groups in the oceans, have been investigated intensively by experiments under elevated CO_2 [see the review by

Meyer and Riebesell (2015) and references therein]. Generally, it is suggested, based on both laboratory studies [see the review by Schlüter *et al.* (2016) and literature therein] and mesocosm investigations (Engel *et al.*, 2005), that OA would inhibit coccolithophore calcification even under varied levels of light, UV, temperature, and nutrients [see the review by Gao *et al.* (2019)], with the exception of a few studies that indicate enhanced calcification and increased coccolith numbers per cell (Iglesias-Rodríguez *et al.*, 2008; White *et al.*, 2018). In terms of production

of particulate organic carbon (POC) and growth, a range of effects of OA has been documented, with POC quota and growth reported as being unaffected or enhanced (Rokitta and Rost, 2012; Mackey et al., 2015; Zhang et al. 2020). OA treatment might reduce the particulate inorganic carbon quota in *Emiliania huxleyi* when grown under different levels of light and nutrients (Zhang et al. 2020). On the other hand, elevated CO₂ tends to enhance the production of transparent exopolymer particles and dissolved organic carbon, which has strong implications for carbon export efficiency (Engel et al., 2004). It should be noticed that most of these results were obtained from short-term experiments simulating OA conditions, which cannot be simply extrapolated to the oceans given the gradual decrease in pH over an extended period of time and interactions of multiple environmental factors.

In recent years, more and more studies have investigated the combined effects of seawater acidification and other environmental factors on *E. huxleyi*. Among these factors, temperature and nutrients seem to play major roles in regulating the physiology of this global important coccolithophore species (Müller et al., 2017; Feng et al., 2018), whereas the lower pH in OA treatments also showed significant impacts on the calcification process (Bodt et al., 2010; Bach et al., 2012). The concurrent changes in CO₂, temperature, and nutrients under future ocean scenarios are supposed to impact the performance of coccolithophores. Decreased growth and primary production with increased exudation of dissolved organic carbon were observed in *E. huxleyi* cells acclimated to elevated CO₂, elevated temperature, and decreased nutrient conditions, leading to the remarkable change in organic carbon partitioning (Borchard and Engel, 2012; Zhang et al., 2020).

For coastal regions, the changes in seawater carbonate chemistry, especially pH and pCO₂, are more complex. Compared with the open ocean, pH fluctuations occur more commonly in coastal seawaters over short time scales from hours to days (Duarte et al., 2013). Such fluctuations in carbonate chemistry of coastal zones are associated with complex interactions between physical and chemical processes as well as biological activities. These processes include tidal cycles, upwellings and nutrient inputs from anthropogenic activities as well as biological removal of CO₂ (Dai et al., 2009; Capone and Hutchins, 2013). Primary producers, both phytoplankton and benthic algae, are photosynthetically active during daytime, resulting in a pH rise, and their respiration leads to a drop in pH during night (Hurd et al., 2011). Such diel variation in some areas can be more than 1 pH unit (Duarte et al., 2013), which well exceeds the value of the pH decrease (~0.4 units) predicted for future OA by the end of this century (Gattuso et al., 2015).

As a consequence of global climate change and intense anthropogenic disturbance, chemical and biological environments in coastal waters are likely to be more variable in the future. On the one hand, the frequency of periodic phytoplankton bloom episodes is likely to increase, during which phytoplankton photosynthesis consumes dissolved inorganic carbon and raises seawater pH (Glibert, 2020). On the other hand, with a declining buffering capacity under elevated pCO₂ condition and increasing aqueous CO₂ released by eutrophication-driven respiration associated with heterotrophic dissimilation of organic matter, coastal waters are suggested to be more susceptible to OA than pelagic waters, with coastal pH dropping faster by about 12% compared to pelagic areas (Cai et al., 2011).

Previous studies usually set two or more steady pCO₂ levels to assess the physiological responses of coccolithophores to future OA scenarios (Hurd et al., 2009). Considering the features of the open ocean as described above, where CO₂ conditions are relative stable, such simulations are reasonable. However, this approach may be inappropriate to mimic the highly variable chemical environment of coastal or upwelling waters (Raven et al., 2020). In addition, it usually overlooks the surrounding micro-layers (i.e. diffusion boundary layer, DBL), a “micro-environment”, which can have major implications for cells, since the DBL could buffer organisms from the chemical changes in milieu (Flynn et al., 2012). Although most coccolithophores are oceanic species, some are also distributed in coastal areas (Godrijan et al., 2018; Matson et al., 2019). Therefore, investigations into coastal species’ responses to OA and exploring the mechanisms involved in coping with fluctuating pH and carbonate chemistry are important to our understanding of effects of global change in inshore waters.

There have been limited studies on the responses of marine phytoplankton to fluctuating pH/pCO₂. Our previous work has shown that the coastal (*Thalassiosira weissflogii*) and oceanic (*Thalassiosira oceanica*) diatoms differed in their capacity to respond to fluctuating carbonate chemistry (Li et al., 2016). After 400 generations’ adaptation under fluctuating high pCO₂, the green alga *Ostreococcus* grew smaller and responded more strongly to further pCO₂ increase than cells under the steady regime (Schaum et al., 2016). For coccolithophores, it has been shown that the calcification rate of an estuarine species, *Pleurochrysis carterae*, increased at elevated pCO₂ when the cells were subjected to diurnally fluctuating carbonate chemistry (White et al., 2018). However, it is still unknown how CO₂ variability affects other coastal coccolithophores. We hypothesized that a coastal strain of *E. huxleyi* could tolerate fluctuating pH/pCO₂, and show different physiological performance compared with cells grown under steady pCO₂ regimes. Hence, in the present study, we manipulated pCO₂ to mimic the diurnally fluctuating carbonate chemistry of the inshore environment in order to investigate the responses of a coastal *E. huxleyi* isolate.

Material and methods

Cultures and experimental setup

Emiliania huxleyi (PML B92/11, originally isolated from coastal waters off Bergen, Norway) was cultured in 500 ml polycarbonate bottles with Aquil medium. The medium was prepared from autoclaved artificial seawater with a salinity of 35, enriched with nitrate, phosphate, trace metal, and vitamin according to Aquil recipes (Sunda et al., 2005). Triplicate monospecific cultures were used for each treatment and were illuminated by cool white fluorescent light at an intensity of 150 μmol photons m⁻² s⁻¹. Cultures were maintained at 15°C, under a 12:12 h light:dark cycle. Semi-continuous methods were used and cells were maintained in exponential growth phase by dilution every 3 d. The maximal concentration during culturing was <50 000 cells ml⁻¹ (Supplementary Figure S1), within which the carbonate chemistry was insignificantly affected by biological activities (Jin et al., 2013).

Emiliania huxleyi was grown under three treatments: (i) steady ambient pCO₂ level (LCs); (ii) steady elevated pCO₂ level (HCs); and (iii) diurnally fluctuating elevated pCO₂ level (HCf) for at least 14 generations (~14 d) before sampling commenced. For

the steady $p\text{CO}_2$ regimes, cultures were bubbled (180 ml min^{-1}) with ambient ($\sim 400\text{ }\mu\text{atm}$, LCs) or high $p\text{CO}_2$ ($\sim 1200\text{ }\mu\text{atm}$, HCs) air respectively, though the exact dissolved CO_2 partial pressures were slightly different ($384 \pm 7\text{ }\mu\text{atm}$ for LCs and $1198 \pm 32\text{ }\mu\text{atm}$ for HCs), which was automatically achieved by using a CO_2 enricher (CE100C, RuiHua). The $p\text{CO}_2$ level of the HCs treatment ($1200\text{ }\mu\text{atm}$) is based on the higher end of predicted values in the Representative Concentration Pathway 8.5 (RCP8.5) emission scenario (IPCC, 2014), and this $p\text{CO}_2$ level also emerges periodically at present in coastal regions (Vargas *et al.*, 2017). The fluctuating $p\text{CO}_2$ regime was obtained by setting different $p\text{CO}_2$ levels at different time periods in the CO_2 enricher. To be specific, we changed the output $p\text{CO}_2$ level every 3 h ($1500\text{ }\mu\text{atm}$ for 0–3 h, $1200\text{ }\mu\text{atm}$ for 3–6 h, $900\text{ }\mu\text{atm}$ for 6–9 h, $600\text{ }\mu\text{atm}$ for 9–12 h after the onset of light and $900\text{ }\mu\text{atm}$ for 0–3 h, $1200\text{ }\mu\text{atm}$ for 3–6 h, $1500\text{ }\mu\text{atm}$ for 6–9 h, $1800\text{ }\mu\text{atm}$ for 9–12 h after the onset of the dark period, Figure 1), so that pH gradually increased during the photoperiod and decreased at night, similar to a typical natural diurnal cycle. The pH/ $p\text{CO}_2$ variation amplitudes of the HCF treatment (0.45 units for pH changes; $1200\text{ }\mu\text{atm}$ for $p\text{CO}_2$ changes) are typical for coastal waters (Duarte *et al.*, 2013). Cultures were diluted in the middle of the photoperiod (6 h after the onset of light), and the replaced media with cells were used for measurement of physiological parameters. On the last day of the experiment, we tested the circadian rhythm of some parameters (mean cell size, seawater carbonate chemistry, maximum and effective photochemical quantum yields, photosynthesis, and calcification rates); subsamples were taken at five time points in the light period, and the culture volume was refilled to 500 ml in the middle of the photoperiod.

Carbonate chemistry sampling and measurements

Samples for total alkalinity (TA) measurements were filtered through cellulose acetate membranes ($0.45\text{ }\mu\text{m}$), poisoned with a saturated HgCl_2 solution, and stored at 4°C . TA was determined by Gran acidimetric titration with a TA analyser (AS-Alk1+, Apollo SciTech). HCl ($\sim 0.1\text{ mol l}^{-1}$) was used to titrate the samples. Certified references (Batch no. 162) from the Scripps Institution of Oceanography were used to assure the precision of the TA measurements ($\pm 2\text{ }\mu\text{mol kg}^{-1}$). TA was determined

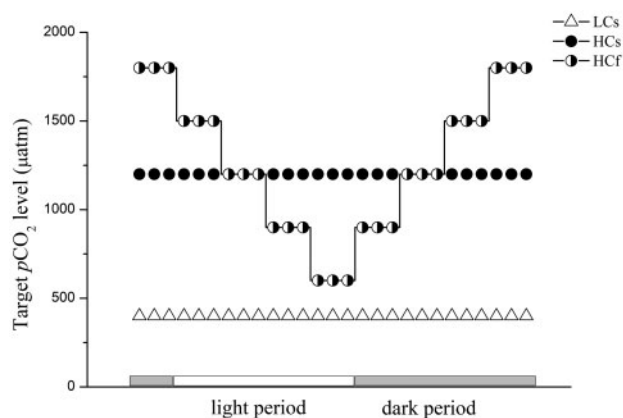


Figure 1. Target $p\text{CO}_2$ levels at different time points in the light and dark period under different carbonate chemistry conditions (LCs, open triangle; HCs, closed circle; HCF, half open/closed circles).

before and after the culture dilutions to investigate the influence of cell metabolism. In addition, samples were collected every 3 h during the light period for the fluctuating $p\text{CO}_2$ regime, and TA was not measured during the dark period. The pH_{NBS} was measured every 3 h during the light period by a pH meter (Orion 2 STAR, Thermo Scientific) calibrated with standard National Bureau of Standards (NBS) buffers. CO2SYS software was used to convert pH_{NBS} values to pH_{T} and calculate other carbonate chemistry parameters based on TA and pH data with the input values of phosphate concentration and salinity being $10\text{ }\mu\text{mol l}^{-1}$ and 35, respectively. Dissociation constants for carbonic acid of Mehrbach *et al.* (1973) refitted by Dickson and Millero (1987) and the dissociation constants for sulphuric acid from Dickson (1990) were chosen for calculations.

Specific growth rate and mean cell size determination

Samples (20 ml) were taken from culture bottles to determine cell abundance and mean cell size using a Coulter Particle Count and Size Analyser (Z2, Beckman Coulter). Specific growth rate was calculated according to the equation: $\mu = (\ln N_1 - \ln N_0) / (t_1 - t_0)$, in which N_1 and N_0 represent cell abundances at t_1 and t_0 .

Chlorophyll and carotenoid contents

Samples for determination of pigment content were filtered onto GF/F filters (25 mm, Whatman) and then extracted overnight in 5 ml of absolute methanol at 4°C in darkness. After centrifugation ($5000g$ for 10 min), the absorption values of the sample supernatants were analysed by a UV-VIS spectrophotometer (DU800, Beckman Coulter). The concentrations of chlorophyll *a* and *c* were calculated according to Ritchie (2006), and carotenoid concentration was determined by the equation of Strickland and Parsons (1972).

Chlorophyll *a* fluorescence

In vivo chlorophyll *a* fluorescence parameters were determined using a multi-colour pulse amplitude modulated fluorometer (MULTI-COLOR-PAM, Walz). Maximum and effective photochemical quantum yields were determined according to the equations given by Genty *et al.* (1989): maximum photochemical quantum yield, $\Phi_{\text{PSII max}} = (F_m - F_0) / F_m$, for dark-adapted (10 min) samples; effective photochemical quantum yield, $\Phi_{\text{PSII eff}} = (F'_m - F_t) / F'_m$ for light-adapted samples. F_m and F'_m indicate the maximum chlorophyll fluorescence of dark and growth-light-adapted samples, respectively; F_0 is the minimum chlorophyll fluorescence of dark-treated cells; and F_t is the steady-state chlorophyll fluorescence of light exposed samples. $\Phi_{\text{PSII eff}}$ was measured under an actinic light intensity ($\sim 180\text{ }\mu\text{mol photons m}^{-2}\text{ s}^{-1}$) similar to culture light levels. The saturation pulse was set at $5000\text{ }\mu\text{mol photons m}^{-2}\text{ s}^{-1}$ for 0.8 s. Given the changing pH/ $p\text{CO}_2$ under the fluctuating regime, maximum and effective photochemical quantum yields were measured every 2 or 3 h, respectively, in the light period.

In addition, rapid light curves were determined in the middle of the light period with 10 progressively increasing actinic light intensities (32, 49, 100, 187, 340, 616, 948, 1330, 1816, $2463\text{ }\mu\text{mol photons m}^{-2}\text{ s}^{-1}$) for 20 s. Maximal relative electron transport rates ($r\text{ETR}_{\text{max}}$), apparent photon transfer efficiency (α), and the light saturation point (I_k) were fitted according the equation of Eilers and Peeters (1988). Since coccoliths of *E. huxleyi* were shown to play an important role in mitigating high light stress to

the cells (Xu et al., 2016), the relative photoinhibition ratio for rETR (Inh) was evaluated here by the following equation: $\text{Inh} (\%) = (\text{rETR}_{\text{max}} - \text{rETR}_x) / \text{rETR}_{\text{max}} \times 100\%$, where rETR_x represents rETR at $2463 \mu\text{mol photons m}^{-2} \text{s}^{-1}$ actinic light intensity.

Determination of photosynthetic and calcification rates

Two subsamples for each culture were used to determine the photosynthetic carbon fixation and calcification rates. Cells were collected and dispensed into borosilicate bottles (20 ml) and inoculated with $5 \mu\text{Ci}$ (0.185 MBq) of $\text{NaH}^{14}\text{CO}_3$ (ICN Radiochemicals). After 60 min of incubation under the same light and temperature conditions as the cultures, samples were gently filtered under dim light onto GF/F filters (25 mm, Whatman) and rinsed with unlabelled medium. One filter, without HCl treatment, was used for determination of total carbon assimilated, including organic carbon fixed by photosynthesis and calcium carbonate produced by calcification. The other filter was fumed with HCl to remove inorganic ^{14}C (contributed by calcification) for measurement of the photosynthetic carbon fixation rate. The filters were then dried (60°C , 5 h) and 5 ml scintillation cocktail was added before assimilated radiocarbon was counted in a liquid scintillation counter (Tri-Carb 2800TR, PerkinElmer). The inorganic ^{14}C contributed by calcification was estimated as the difference between the CPM (counts per minute) values of the two filters with/without exposure to HCl fumes, and the calcification rate was calculated from the inorganic ^{14}C content and cell abundance (Xu et al., 2020):

$$\text{calcification rate} = \frac{\text{CPMT} - \text{CPMP}}{C_e} \times I_f \times \frac{1}{A \times \text{cell concentration} \times \text{time}},$$

where CPM_T and CPM_P represent ^{14}C activities of total (photosynthetic fixation plus calcification) and photosynthetic fixation, respectively, C_e is the counting efficiency of the liquid scintillation counter, I_f is the isotope discrimination factor, DIC is the total dissolved inorganic carbon in cultures and A is the total ^{14}C activity added to each sample. The main uncertainty of this method might be whether the time of the HCl fume treatment is enough to remove all the inorganic carbon on the filters. To minimize such error, in the present study, we fumed the filters with HCl overnight.

Cell abundances at each time point were determined to calculate carbon fixation rates per cell. In order to monitor the diurnal change in photosynthetic and calcification rates, ^{14}C incubations were done every 2–3 h during the light period. Daily photosynthetic carbon fixation rate was calculated by multiplying the mean of rates determined at five time points by 12 (the duration of the light period). As the calcification of *E. huxleyi* is typically light dependent (Linschooten et al., 1991; Müller et al., 2008), daily calcification rate was also calculated as above.

Statistical analyses

Data were analysed using SPSS statistics 22 and reported as means \pm SD. Homogeneity of variance and normality of data was tested before performing parametric tests. One-way ANOVA and *post hoc* Tukey's tests were used to determine differences among $p\text{CO}_2$ treatments with a significance level of $p < 0.05$.

Results

Carbonate chemistry in the experimental regimes

The carbonate chemistry was relatively stable under LCs and HCs treatments where pH_T values were 8.00 ± 0.01 and 7.54 ± 0.01 , respectively (Table 1). In the steady regimes, changes in DIC and TA caused by biological activities were $< 3\%$ before and after the culture dilution, with the pH change being < 0.03 units. The pH variation range in the HcF treatment was 0.45. At the beginning of the light period, the pH_T was the lowest, with a value of 7.36 ± 0.01 , which increased to 7.54 ± 0.01 at 6 h after the onset of the light, similar to the value in the HCs regime. After that, the pH reached its highest value at the end of the photoperiod, at around pH_T 7.81 and then gradually decreased in the dark period, finally completing a fluctuation cycle. During the photoperiod, decreasing DIC and CO_2 in the HcF culture was observed over time as expected from the treatment regimes.

Specific growth rate, cell size, and pigment content

For the steady regime, elevated $p\text{CO}_2$ did not show any effects on specific growth rate ($p = 0.945$). The fluctuating carbonate chemistry enhanced growth rates of cells compared with the steady regime, including both LCs and HCs treatments (one-way ANOVA, $p = 0.018$, Figure 2). The growth rate under the HcF treatment was 32% higher than that under HCs.

An increased trend of mean cell size in all treatments was observed from the beginning to the end of the light period (Figure 3). While there were no differences between the two steady treatments, HcF cells were smaller compared with LCs and HCs cells except for the time point at the end of light period ($p = 0.009, 0.033, 0.041, \text{ and } 0.007$ for the four earlier time points, respectively). There were no significant differences in pigment content, including Chl *a*, Chl *c*, and carotenoids, across the different $p\text{CO}_2$ treatments ($p = 0.497, 0.498, \text{ and } 0.163$ for Chl *a*, Chl *c*, and carotenoids respectively, Table 2).

Chlorophyll *a* fluorescence

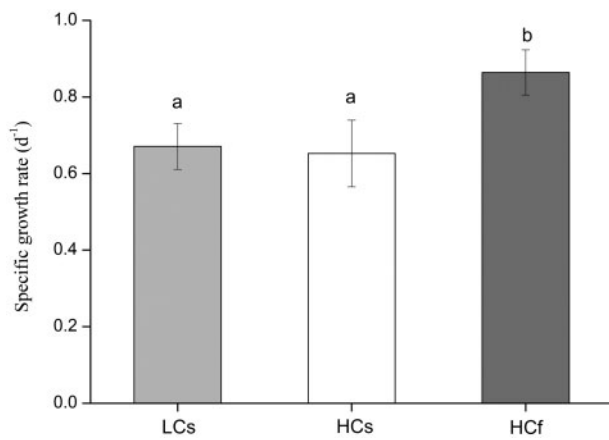
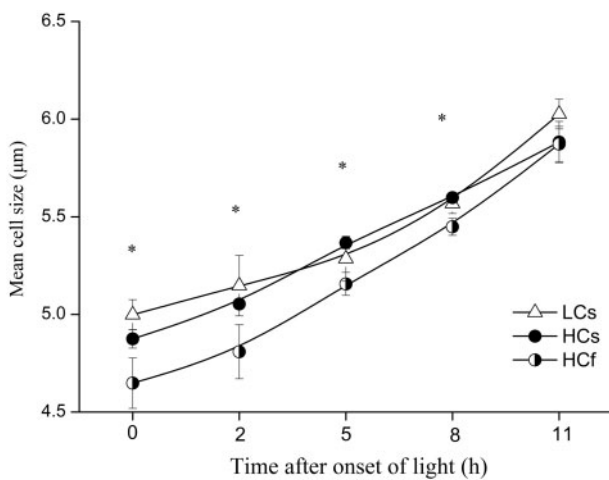
While there were no significant differences in relative photoinhibition ratio of rETR among the three treatments, cells grown under the LCs condition showed significantly higher rETR_{max} and α than HCs and HcF grown ones. The fluctuating regime stimulated the electron transport rate compared with the steady regime under HC (Figure 4). The rETR_{max} of cells grown under the HcF treatment was 11% higher than that of the HCs treatment ($p < 0.001$), with a 16% higher I_k observed at the same time (Table 3).

The time courses of $\Phi_{\text{PSII max}}$ and $\Phi_{\text{PSII eff}}$ during the light period were different among the different $p\text{CO}_2$ treatments (Figure 5). The values of $\Phi_{\text{PSII max}}$ under the LCs and HcF treatments were relatively constant in the first half of the light period, then increased to around 0.57 at the end of the photoperiod. In contrast, HCs cells showed the highest $\Phi_{\text{PSII max}}$ in the middle of the light period and the values were generally lower than those for cells under the other two treatments. For effective photochemical quantum yield, LCs cells always showed the highest values and HCs consistently had the lowest values among the three treatments. A generally increased trend of $\Phi_{\text{PSII eff}}$ values over the light period was observed for HcF cells, although cells in the other two treatments showed peak values in the middle of light period.

Table 1. Carbonate chemistry parameters of culture media under steady ambient $p\text{CO}_2$ (LCs), steady elevated $p\text{CO}_2$ (HCs), and diurnally fluctuating elevated $p\text{CO}_2$ (HCF).

Treatment	pH_T	TA ($\mu\text{mol kg}^{-1}$)	DIC ($\mu\text{mol kg}^{-1}$)	HCO_3^- ($\mu\text{mol kg}^{-1}$)	CO_3^{2-} ($\mu\text{mol kg}^{-1}$)	CO_2 ($\mu\text{mol kg}^{-1}$)
LCs	8.00 ± 0.01^a	$1\,939.95 \pm 2.78^a$	$1\,751.01 \pm 2.62^a$	$1\,615.07 \pm 2.42^a$	122.06 ± 0.18^a	13.88 ± 0.02^a
HCs	7.54 ± 0.01^b	$2\,009.45 \pm 6.34^b$	$1\,971.60 \pm 6.65^b$	$1\,875.96 \pm 6.33^b$	48.41 ± 0.61^b	47.22 ± 0.69^b
HCF 0 h	7.36 ± 0.01^c	$1\,982.59 \pm 28.02^{ab}$	$1\,992.78 \pm 28.57^b$	$1\,889.20 \pm 27.08^b$	32.71 ± 0.47^c	70.88 ± 1.02^c
HCF 3 h	7.45 ± 0.01^d	$1\,994.52 \pm 8.83^b$	$1\,978.79 \pm 7.32^b$	$1\,881.46 \pm 7.17^b$	40.39 ± 0.69^d	56.94 ± 0.54^d
HCF 6 h	7.54 ± 0.02^b	$2\,006.45 \pm 21.54^b$	$1\,967.64 \pm 17.27^b$	$1\,872.16 \pm 16.39^b$	48.71 ± 2.13^b	46.77 ± 1.24^b
HCF 9 h	7.72 ± 0.01^e	$2\,004.01 \pm 14.70^b$	$1\,911.89 \pm 14.38^c$	$1\,810.43 \pm 13.62^c$	71.81 ± 0.54^e	29.65 ± 0.22^e
HCF 12 h	7.81 ± 0.01^f	$2\,011.37 \pm 16.12^b$	$1\,891.08 \pm 15.72^c$	$1\,780.95 \pm 14.92^c$	86.24 ± 1.24^f	23.89 ± 0.40^f

For HCF treatment, TA and pH were determined at different time points in the light period (0, 3, 6, 9, and 12 h after the onset of light). The pH_{NBS} values were converted to pH_T with the CO2SYS software. Values are the means \pm SD of triplicate cultures. Different superscripted letters indicate significant ($p < 0.05$) differences among treatments.

**Figure 2.** Specific growth rates of *E. huxleyi* cells grown under steady ambient $p\text{CO}_2$ (LCs, light grey bar), steady elevated $p\text{CO}_2$ (HCs, white bar), and diurnally fluctuating elevated $p\text{CO}_2$ (HCF, grey bar). Values are the means \pm SD of triplicate cultures. The different letters indicate significant ($p < 0.05$) differences among treatments.**Figure 3.** Mean cell size of *E. huxleyi* cells grown under different carbonate chemistry conditions (LCs, open triangle; HCs, closed circle; HCF, half open/closed circle) determined at different time points in the light period. Values are the means \pm SD of triplicate cultures. Asterisks indicate significant ($p < 0.05$) differences among treatments.

Photosynthesis and calcification rates

After the onset of light, the photosynthesis rate of cells grown under the HCF treatment increased with time and reached a maximum ($1.09 \pm 0.27 \text{ pg C cell}^{-1} \text{ h}^{-1}$) in the middle of the light period and was maintained at this rate until the light was turned off; LCs and HCs cells showed a similar trend to that of HCF cultures, though lower photosynthetic rates than those of HCF cells were found at two time points during the light period (Figure 6a).

No significant time-related trends in the calcification rates could be observed for HCs and HCF cells as a result of quite large standard deviation values, while an increase in calcification rate over time was found for LCs cells (Figure 6b). The calcification rate reached a maximum at the end of the photoperiod under the LCs treatment, attaining a value of $1.66 \pm 0.34 \text{ pg C cell}^{-1} \text{ h}^{-1}$. Overall, there were no significant differences in calcification rates among three $p\text{CO}_2$ treatments during the photoperiod with the exceptions that cells grown under the HCs condition had a higher rate in the middle of the light period and LCs cells showed maximum calcification rate at the end of the light period.

A fluctuating regime at elevated $p\text{CO}_2$ enhanced the mean value of daily photosynthesis rate, although the increase was not statistically significant ($p = 0.062$, Figure 7a). In contrast, LCs cells had the highest daily calcification rate ($11.8 \pm 0.7 \text{ pg C cell}^{-1} \text{ d}^{-1}$), which was 36% ($p = 0.003$) and 46% ($p = 0.001$) higher than that of cells under the HCs and HCF treatments, respectively (Figure 7b). Therefore, the highest C/P ratio was observed under the LCs treatment, with a value about 1.5, and no significant differences in the ratio were detected for the steady and fluctuating regimes (Figure 7c).

Discussion

Our findings demonstrated that fluctuations in $p\text{CO}_2$ had a positive effect on the growth of *E. huxleyi*, with enhanced photosynthetic rates in the middle and at the end of the light period along with stimulated (by about 11%) energy transfer as reflected in the electron transport rate. These results indicate that this *E. huxleyi* strain can increase energy supply to cope with diurnal pH changes and benefit from the elevated CO_2 concentration for growth.

Emiliania huxleyi strains are known to be capable of establishing a new physiological equilibrium through changes in rates of various essential processes in $< 24 \text{ h}$ when exposed to contrasting different environmental changes (Barcelos e Ramos *et al.*,

Table 2. Pigment contents of *E. huxleyi* cells grown under different carbonate chemistry conditions [LCs, steady ambient $p\text{CO}_2$ (LCs); HCs, steady elevated $p\text{CO}_2$; Hcf, diurnally fluctuating elevated $p\text{CO}_2$].

$p\text{CO}_2$ treatment	Chlorophyll <i>a</i> content (pg cell ⁻¹)	Chlorophyll <i>c</i> content (pg cell ⁻¹)	Carotenoid content (pg cell ⁻¹)
LCs	0.12 ± 0.02 ^a	0.04 ± 0.01 ^a	0.13 ± 0.01 ^a
HCs	0.12 ± 0.01 ^a	0.04 ± 0.01 ^a	0.14 ± 0.01 ^a
Hcf	0.13 ± 0.01 ^a	0.03 ± 0.01 ^a	0.15 ± 0.01 ^a

Values are the means ± SD of triplicate cultures. Different superscripted letters indicate significant ($p < 0.05$) differences among treatments.

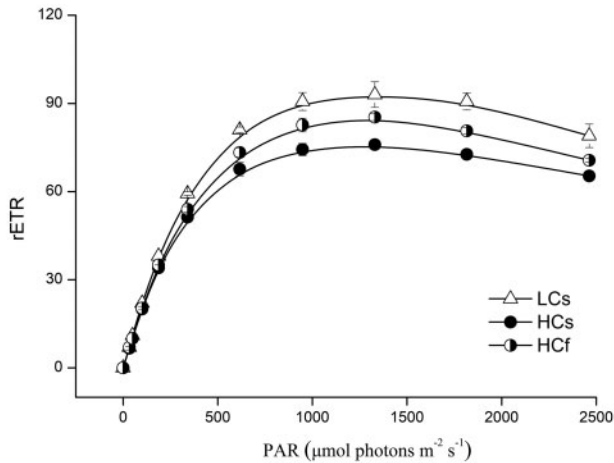


Figure 4. Rapid light curves of *E. huxleyi* cells grown under different carbonate chemistry conditions (LCs, open triangle; HCs, closed circle; Hcf, half open/closed circle). Values are the means ± SD of triplicate cultures.

2010). Additionally, an *E. huxleyi* strain isolated from a Norwegian fjord has been shown to be more tolerant to low pH than strains isolated from waters near the Azores and Canary Islands (Zhang et al., 2018), which was attributed to the larger $p\text{CO}_2$ and pH variability in coastal waters off Bergen compared with the rather stable oceanic conditions at the other two sites (Omar et al., 2010). These results are consistent with the reported results for a coastal diatom, *T. weissflogii* (Li et al., 2016). As mirrored in the present study and other works (Li et al., 2016; White et al., 2018), coastal phytoplankton isolates may be less sensitive to, and even benefit from, dynamic carbonate chemistry compared with oceanic strains. The findings, reported in this work, that growth of *E. huxleyi* was enhanced under diel fluctuation of elevated $p\text{CO}_2$ might be a partial explanation for the high abundance of coccolithophores in coastal sediments (Cheng and Wang, 1997). However, some field studies have shown that coccolithophores do not necessarily exhibit adaptations to naturally high CO_2 waters (Dassow et al., 2018). Thus, more studies are needed to clarify the adaptations of coccolithophores to OA and fluctuating pH.

The pH_T under the fluctuating regime gradually decreased to around 7.36 before the onset of the light period (Table 1), an acidified environment would promote respiration (Bach et al., 2011; Jin et al., 2015; Meyer and Riebesell, 2015). This could further lower pH within the DBL surrounding the cells (Flynn et al., 2012). Energy generated from enhanced respiration at decreased pH might be re-allocated to maintain intracellular acid-base homeostasis, considering that the intracellular pH of *E. huxleyi* decreases as seawater pH decreases (Suffrian et al., 2011). The

enhanced respiration could also be related to the higher growth under the fluctuating regime, as this process generates ATP and carbon skeletons for growth (Raven and Beardall, 2005).

Many coastal calcifying organisms could adapt to large pH fluctuations in their habitats in ways that mitigate the negative effects on calcification of lowered pH under OA conditions (Hendriks et al., 2015). For example, the bivalve *Pinna nobilis* inhabits Mediterranean seagrass meadows, where pH inside the meadow is 0.3–0.5 units higher than the surrounding seawater during the daytime, and this is beneficial for its calcification (Hendriks et al., 2014). Other bivalves, such as the mussel *Mytilus edulis*, could utilize their body fluids such as extrapallial fluid or haemolymph, a set of internal buffering systems, to avoid lower pH at calcification sites (Heinemann et al., 2013). Scleractinian corals could manipulate the pH of the calcifying fluid by Ca^{2+} -ATPase pumping of calcium ions in exchange for protons, and this acts as a form of extracellular regulation of pH (Allemand et al., 2004). This mechanism is beneficial to calcification of corals, as shown by Dufault et al. (2012), who found that a fluctuating $p\text{CO}_2$ regime could enhance the calcification of the coral *Seriatopora caliendrum*.

In contrast, *E. huxleyi*, as a unicellular phytoplankter without a host, lacks complex structures such as the extrapallium of bivalves or the blastophyllum of corals. Moreover, the surface conditions of nano-phytoplankton like *E. huxleyi*, with an equivalent spherical diameter $< 5 \mu\text{m}$, are close to bulk-water conditions, due to the positive relationship between cell size and the thickness of the DBL (Wolf-Gladrow and Riebesell, 1997; Flynn et al., 2012). That is to say, *E. huxleyi* cells distributed in the coastal seawater are directly exposed to the fluctuating carbonate chemistry environment with little buffering effect of a DBL. Thus, *E. huxleyi* could adopt different strategies in calcification to respond to fluctuating pH. As shown in the present study, seawater acidification treatment depressed the daily calcification rates regardless of the steady or fluctuating regime (Figure 7b). In accordance with the calcification rate, lower C/P (calcification to photosynthesis) was also detected at elevated $p\text{CO}_2$ level (Figure 7c). These results are consistent with a large body of studies (Meyer and Riebesell, 2015) and the pattern of decreasing calcification with increasing $p\text{CO}_2$ and concomitant decreasing CO_3^{2-} concentration has been verified by an observational and paleo study (Beaufort et al., 2011). However, for the estuarine coccolithophore *P. carterae*, an elevated mean $p\text{CO}_2$ of 750 μatm promoted calcification and C/P compared to the current $p\text{CO}_2$ level (White et al., 2018). The different responses to decreased and fluctuating pH might be caused by the complex interactions of multiple factors and species-specificity as shown in two ecologically dominant non-CCM (carbon dioxide concentrating mechanism) red macroalgae (Britton et al., 2019). Changes in C/P would impact the CO_2 exchange between surface ocean and atmosphere and the export of organic carbon to the deep ocean. At elevated $p\text{CO}_2$ level, *E. huxleyi* cells

Table 3. The maximal rate of rETR (rETR_{max}), apparent photon transfer efficiency (α) and the light saturation point [I_k (μmol photons m⁻² s⁻¹)] derived from rapid light curves of *E. huxleyi* cells grown under different carbonate chemistry conditions.

pCO ₂ treatment	rETR _{max}	α	I _k (μmol photons m ⁻² s ⁻¹)	Inhibition ratio (%)
LCs	93.40 ± 3.35 ^a	0.243 ± 0.01 ^a	385 ± 20 ^a	15 ± 2 ^a
HCs	76.08 ± 1.34 ^b	0.230 ± 0.01 ^b	331 ± 7 ^b	14 ± 2 ^a
HCF	84.68 ± 1.20 ^c	0.221 ± 0.01 ^b	383 ± 10 ^a	17 ± 2 ^a

The relative photoinhibition ratio for rETR was evaluated here by the following equation: Inh (%) = (rETR_{max} - rETR_x) / rETR_{max} × 100%. Values are the means ± SD of triplicate cultures. Different superscripted letters indicate significant (p < 0.05) differences among treatments.

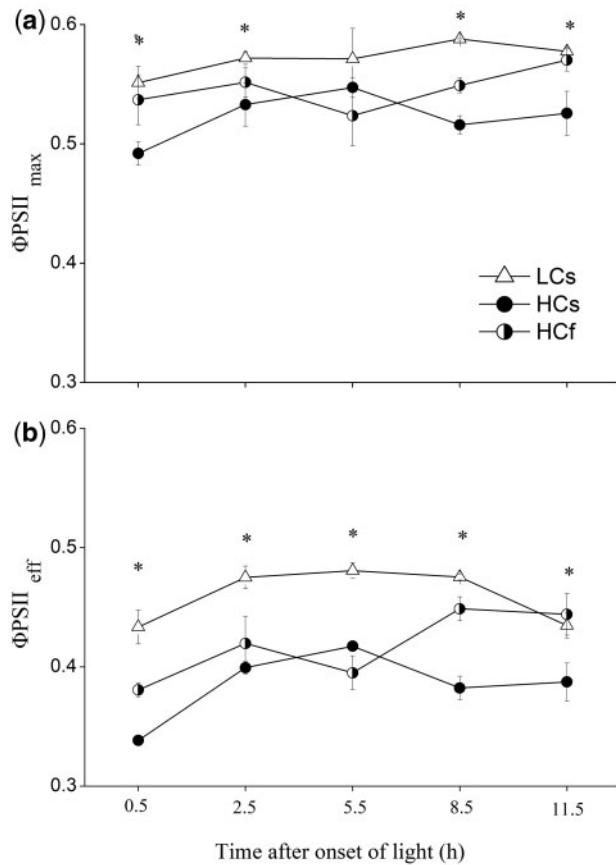


Figure 5. Maximum (a) and effective photochemical quantum yields (b) of *E. huxleyi* cells grown under different carbonate chemistry conditions (LCs, open triangle; HCs, closed circle; HCF, half open/closed circle) determined at different time points in the light period. Values are the means ± SD of triplicate cultures. Asterisks indicate significant (p < 0.05) differences among treatments.

calcified less and produced similar amounts of organic carbon as the cells were grown at ambient pCO₂ level, which might lead to decreased sinking of cells since sinking rate for coccolithophores is positively related to the ratio of particulate inorganic carbon to organic carbon (Hoffmann *et al.*, 2015). Nevertheless, it should be noted that the results obtained from laboratory studies cannot be simply extrapolated to the real ocean. In contrast to results from most culture studies, the percentage and abundance of overcalcified morphotype of *E. huxleyi* increased in the Bay of Biscay when pH and CaCO₃ saturation are lowest (Smith *et al.*, 2012).

The cell size of *E. huxleyi* cells increased with time irrespective of the CO₂ treatments (Figure 3) and has little to do with changes

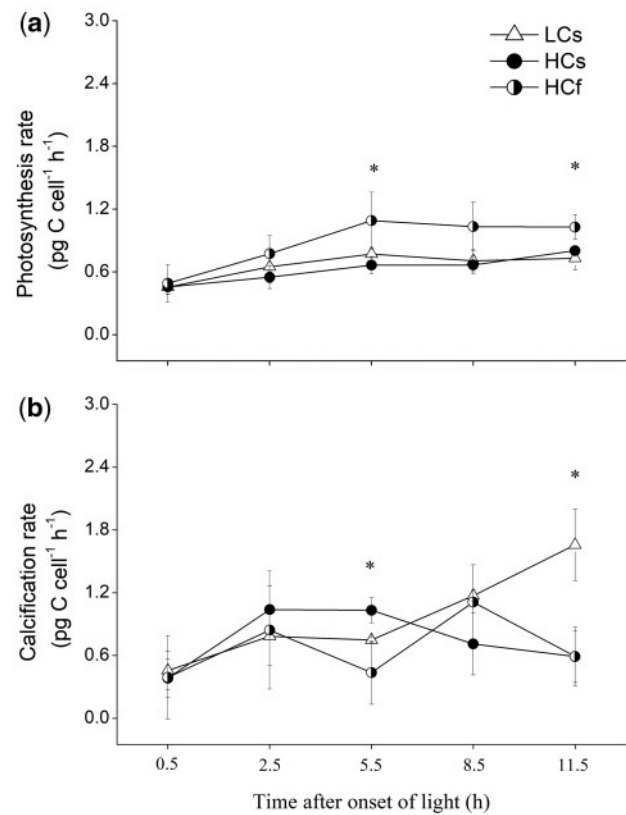


Figure 6. Photosynthesis (a) and calcification (b) rates of *E. huxleyi* cells grown under different carbonate chemistry conditions (LCs, open triangle; HCs, closed circle; HCF, half open/closed circle) determined at different time points in the light period. Values are the means ± SD of triplicate cultures. Asterisks indicate significant (p < 0.05) differences among treatments.

in the calcified layer thickness. Although there were significant differences among the treatments in the early phase of the light period, with the HCF-grown cells being of larger size, the difference becomes smaller and insignificant at the end of light period, implying that the POC quota increased with time during the daytime. Faster assimilation to generate more organic matter under the fluctuating high CO₂ due to enhanced energy transfer is likely to be responsible for the “catch-up” in cell size. Nevertheless, cell division under fluctuating high CO₂ must have resulted in the smaller cells at the time when the light was turned on (Figure 3).

The dynamic nature of coastal waters, especially as regards seawater carbonate chemistry, makes them a special, though generally overlooked, environment. Our findings in the present work,

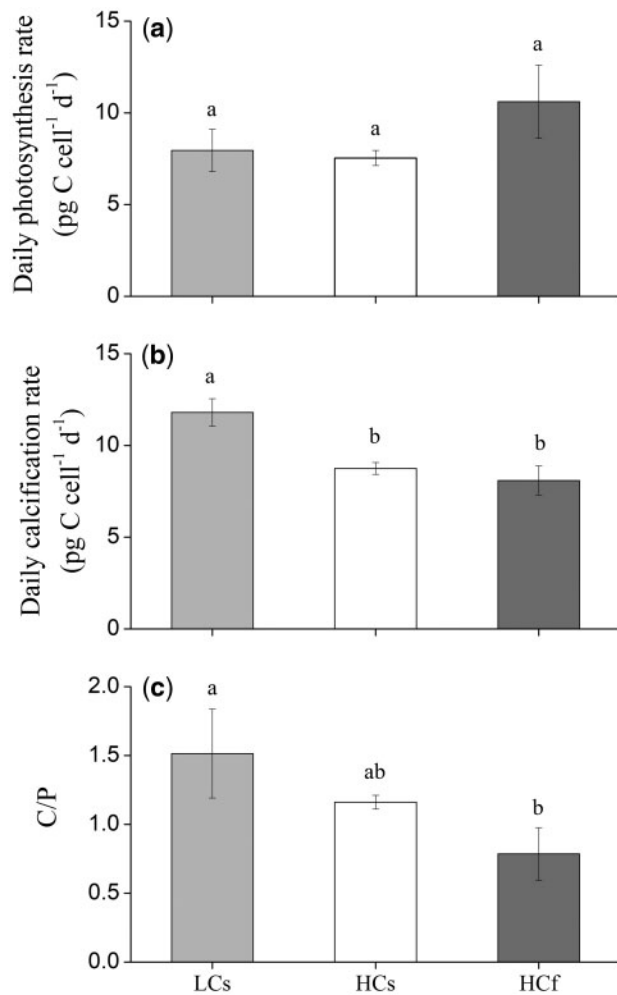


Figure 7. Daily photosynthesis (a) and calcification (b) rates and the ratio of calcification to photosynthesis (c) of *E. huxleyi* cells grown under steady ambient $p\text{CO}_2$ (LCs, light grey bar), steady elevated $p\text{CO}_2$ (HCs, white bar), and diurnally fluctuating elevated $p\text{CO}_2$ (HCf, grey bar). Values are the means \pm SD of triplicate cultures. The different letters indicate significant ($p < 0.05$) differences among treatments.

along with others (Li *et al.* 2016), imply that coastal phytoplankton species or strains show relatively more resilience to reduced pH under OA conditions. With progressive OA, the buffering capacity of seawater decreases as dissolved inorganic carbon increases, which would enhance the amplitude of pH variation in coastal waters (Egleston *et al.*, 2010). More energy for coastal phytoplankton cells to maintain intracellular pH homeostasis would be required, especially during night time when respiration exacerbates acidification. However, the beneficial effects from elevated CO_2 during daytime might counteract the acidification stress, as shown in our work with *E. huxleyi*. It should be kept in mind that these results were based on a short-term experiment (~ 14 generations) and a single strain culture. The species, and even strain, specificity (Langer *et al.*, 2009) and adaptive evolution (Lohbeck *et al.*, 2012) need to be taken into account when predicating the overall responses of coccolithophores to OA. Nevertheless, basic investigations such as the present study are the first step to understand the effects of fluctuating seawater

carbonate chemistry, and there is an urgent need for studies on more species.

Supplementary data

Supplementary material is available at the ICESJMS online version of the manuscript.

Data availability

The data underlying this article will be shared on reasonable request to the corresponding author.

Acknowledgements

This research has been supported by National Natural Science Foundation of China (41720104005 and 41721005) and China Postdoctoral Science Foundation (2019M661766).

References

- Allemand, D., Ferrier-Pagès, C., Furla, P., Houlbrèque, F., Puverel, S., Reynaud, S., Tambutté, É. *et al.* 2004. Biomineralisation in reef-building corals: from molecular mechanisms to environmental control. *Comptes Rendus Palevol*, 3: 453–467.
- Bach, L. T., Bauke, C., Meier, K. J. S., Riebesell, U., and Schulz, K. G. 2012. Influence of changing carbonate chemistry on morphology and weight of coccoliths formed by *Emiliania huxleyi*. *Biogeosciences*, 9: 3449–3463.
- Bach, L. T., Riebesell, U., and Schulz, K. G. 2011. Distinguishing between the effects of ocean acidification and ocean carbonation in the coccolithophore *Emiliania huxleyi*. *Limnology and Oceanography*, 56: 2040–2050.
- Barcelos e Ramos, J., Müller, M. N., and Riebesell, U. 2010. Short-term response of the coccolithophore *Emiliania huxleyi* to an abrupt change in seawater carbon dioxide concentrations. *Biogeosciences*, 7: 177–186.
- Bodt, C. D., Oostende, N. V., Harlay, J., Sabbe, K., and Chou, L. 2010. Individual and interacting effects of $p\text{CO}_2$ and temperature on *Emiliania huxleyi* calcification: study of the calcite production, the coccolith morphology and the coccosphere size. *Biogeosciences*, 7: 1401–1412.
- Borchard, C., and Engel, A. 2012. Organic matter exudation by *Emiliania huxleyi* under simulated future ocean conditions. *Biogeosciences*, 9: 3405–3423.
- Beaufort, L., Probert, I., de Garidel-Thoron, T., Bendif, E. M., Ruiz-Pino, D., Metzl, N., Goyet, C. *et al.* 2011. Sensitivity of coccolithophores to carbonate chemistry and ocean acidification. *Nature*, 476: 80–83.
- Britton, D., Mundy, C. N., McGraw, C. M., Revill, A. T., and Hurd, C. L. 2019. Responses of seaweeds that use CO_2 as their sole inorganic carbon source to ocean acidification: differential effects of fluctuating pH but little benefit of CO_2 enrichment. *ICES Journal of Marine Science*, 76: 1860–1870.
- Cai, W.-J., Hu, X., Huang, W.-J., Murrell, M. C., Lehrter, J. C., Lohrenz, S. E., Chou, W.-C., *et al.* 2011. Acidification of subsurface coastal waters enhanced by eutrophication. *Nature Geoscience*, 4: 766–770.
- Capone, D. G., and Hutchins, D. A. 2013. Microbial biogeochemistry of coastal upwelling regimes in a changing ocean. *Nature Geoscience*, 6: 711–717.
- Cheng, X., and Wang, P. 1997. Controlling factors of coccolith distribution in surface sediments of the China seas: marginal sea nanofossil assemblages revisited. *Marine Micropaleontology*, 32: 155–172.
- Dai, M., Lu, Z., Zhai, W., Chen, B., Cao, Z., Zhou, K., Cai, W. *et al.* 2009. Diurnal variations of surface seawater $p\text{CO}_2$ in contrasting coastal environments. *Limnology and Oceanography*, 54: 735–745.

- Dassow, P. V., Díaz-Rosas, F., Bendif, E. M., Gaitán-Espitia, J. D., Mella-Flores, D., Rokitta, S., John, U. *et al.* 2018. Over-calcified forms of the coccolithophore *Emiliana huxleyi* in high-CO₂ waters are not preadapted to ocean acidification. *Biogeosciences*, 15: 1515–1534.
- Dickson, A. G. 1990. Standard potential of the reaction: AgCl(s) + 1/2H₂(g) = Ag(s) + HCl(aq), and the standard acidity constant of the ion HSO₄⁻ in synthetic seawater from 273.15 to 318.15 K. *Journal of Chemical Thermodynamics*, 22: 113–127.
- Dickson, A. G., and Millero, F. J. 1987. A comparison of the equilibrium constants for the dissociation of carbonic acid in seawater media. *Deep Sea Research Part I-Oceanographic Research Papers*, 34: 1733–1743.
- Duarte, C. M., Hendriks, I. E., Moore, T. S., Olsen, Y. S., Steckbauer, A., Ramajo, L., Carstensen, J. *et al.* 2013. Is ocean acidification an open-ocean syndrome? Understanding anthropogenic impacts on seawater pH. *Estuaries & Coasts*, 36: 221–236.
- Dufault, A. M., Cumbo, V. R., Fan, T. Y., and Edmunds, P. J. 2012. Effects of diurnally oscillating pCO₂ on the calcification and survival of coral recruits. *Proceedings of the Royal Society B: Biological Sciences*, 279: 2951–2958.
- Egleston, E. S., Sabine, C. L., and Morel, F. M. M. 2010. Revelle revisited: buffer factors that quantify the response of ocean chemistry to changes in DIC and alkalinity. *Global Biogeochemical Cycles*, 24: GB1002.
- Engel, A., Delille, B., Jacquet, S., Riebesell, U., Rochelle-Newall, E., Terbrüggen, A., and Zondervan, I. 2004. Transparent exopolymer particles and dissolved organic carbon production by *Emiliana huxleyi* exposed to different CO₂ concentrations. *Aquatic Microbial Ecology*, 34: 93–104.
- Engel, A., Zondervan, I., Aerts, K., Beaufort, L., Benthien, A., Chou, L., Delille, B. *et al.* 2005. Testing the direct effect of CO₂ concentration on a bloom of the coccolithophorid *Emiliana huxleyi* in mesocosm experiments. *Limnology and Oceanography*, 50: 493–507.
- Eilers, P., and Peeters, J. 1988. A model for the relationship between light intensity and the rate of photosynthesis in phytoplankton. *Ecological Modelling*, 42: 199–215.
- Feng, Y., Roleda, M. Y., Armstrong, E., Law, C. S., Boyd, P. W., and Hurd, C. L. 2018. Environmental controls on the elemental composition of a Southern Hemisphere strain of the coccolithophore *Emiliana huxleyi*. *Biogeosciences*, 15: 581–595.
- Flynn, K. J., Blackford, J. C., Baird, M. E., Raven, J. A., Clark, D. R., Beardall, J., Brownlee, C. *et al.* 2012. Changes in pH at the exterior surface of plankton with ocean acidification. *Nature Climate Change*, 2: 510–513.
- Gattuso, J. P., Magnan, A., Bille, R., Cheung, W. W., Howes, E. L., Joos, F., Allemand, D. *et al.* 2015. Contrasting futures for ocean and society from different anthropogenic CO₂ emissions scenarios. *Science*, 349: aac4722.
- Genty, B., Briantais, J. M., and Baker, N. R. 1989. The relationship between the quantum yield of photosynthetic electron transport and quenching of chlorophyll fluorescence. *Biochimica et Biophysica Acta (BBA)-General Subjects*, 990: 87–92.
- Gao, K., Beardall, J., Häder, D. P., Hall-Spencer, J. M., Gao, G., and Hutchins, D. A. 2019. Effects of ocean acidification on marine photosynthetic organisms under the concurrent influences of warming, UV radiation, and deoxygenation. *Frontiers in Marine Science*, 6: 322.
- Glibert, P. M. 2020. Harmful algae at the complex nexus of eutrophication and climate change. *Harmful Algae*, 91: 101583.
- Godrijan, J., Young, J. R., Pfannkuchen, D. M., Precali, R., and Pfannkuchen, M. 2018. Coastal zones as important habitats of coccolithophores: a study of species diversity, succession, and life-cycle phases. *Limnology and Oceanography*, 63: 1692–1710.
- Heinemann, A., Fietzke, J., Melzner, F., Böhm, F., Thomsen, J., Garbe log Chönberg, D., and Eisenhauer, A. 2013. Conditions of *Mytilus edulis* extracellular body fluids and shell composition in a pH-treatment experiment: acid-base status, trace elements and δ¹¹B. *Geochemistry Geophysics Geosystems*, 13: Q01005.
- Hendriks, I. E., Duarte, C. M., Olsen, Y. S., Steckbauer, A., Ramajo, L., Moore, T. S., Trotter, J. A. *et al.* 2015. Biological mechanisms supporting adaptation to ocean acidification in coastal ecosystems. *Estuarine, Coastal and Shelf Science*, 152: A1–A8.
- Hendriks, I. E., Olsen, Y. S., Ramajo, L., Basso, L., Steckbauer, A., Moore, T. S., Howard, J. *et al.* 2014. Photosynthetic activity buffers ocean acidification in seagrass meadows. *Biogeosciences*, 11: 333–346.
- Hoffmann, R., Kirchlechner, C., Langer, G., Wochnik, A. S., Griesshaber, E., Schmahl, W. W., and Scheu, C. 2015. Insight into *Emiliana huxleyi* coccospheres by focused ion beam sectioning. *Biogeosciences*, 12: 825–834.
- Hurd, C. L., Cornwall, C. E., Currie, K., Hepburn, C. D., McGraw, C. M., Hunter, K. A., and Boyd, P. W. 2011. Metabolically induced pH fluctuations by some coastal calcifiers exceed projected 22nd century ocean acidification: a mechanism for differential susceptibility? *Global Change Biology*, 17: 3254–3262.
- Hurd, C. L., Hepburn, C. D., Currie, K. I., Raven, J. A., and Hunter, K. A. 2009. Testing the effects of ocean acidification on algal metabolism: considerations for experimental designs. *Journal of Phycology*, 45: 1236–1251.
- Iglesias-Rodriguez, M. D., Halloran, P. R., Rickaby, R. E. M., Hall, I. R., Colmenero-Hidalgo, E., Gittins, J. R., Green, D. R. H. *et al.* 2008. Phytoplankton calcification in a high-CO₂ world. *Science*, 320: 336–340.
- IPCC. 2014. *Climate Change 2014: Synthesis Report. Contribution of working groups I, II and III to the fifth assessment report of the intergovernmental panel on climate change.* IPCC, Geneva.
- Jin, P., Gao, K., Villafañe, V. E., Campbell, D. A., and Helbling, E. W. 2013. Ocean acidification alters the photosynthetic responses of a coccolithophorid to fluctuating ultraviolet and visible radiation. *Plant Physiology*, 162: 2084–2094.
- Jin, P., Wang, T., Liu, N., Dupont, S., Beardall, J., Boyd, P. W., Riebesell, U. *et al.* 2015. Ocean acidification increases the accumulation of toxic phenolic compounds across trophic levels. *Nature Communications*, 6: 8714.
- Langer, G., Nehrke, G., Probert, I., Ly, J., and Ziveri, P. 2009. Strain-specific responses of *Emiliana huxleyi* to changing seawater carbonate chemistry. *Biogeosciences*, 6: 2637–2646.
- Li, F., Wu, Y., Hutchins, D. A., Fu, F., and Gao, K. 2016. Physiological responses of coastal and oceanic diatoms to diurnal fluctuations in seawater carbonate chemistry under two CO₂ concentrations. *Biogeosciences*, 13: 6247–6259.
- Linschooten, C., Bleijswijk, J. D. L. V., Emburg, P. R. V., Vrind, J. P. M. D., Kempers, E. S., Westbroek, P., and Jong, V. D. 1991. Role of the light-dark cycle and medium composition on the production of coccoliths by *Emiliana huxleyi* (Haptophyceae). *Journal of Phycology*, 27: 82–86.
- Lohbeck, K. T., Riebesell, U., and Reusch, T. B. H. 2012. Adaptive evolution of a key phytoplankton species to ocean acidification. *Nature Geosciences*, 5: 346–351.
- Mackey, K. R. M., Morris, J. J., Morel, F. M. M., and Kranz, S. A. 2015. Response of photosynthesis to ocean acidification. *Oceanography*, 28: 2.
- Matson, P. G., Washburn, L., Fields, E. A., Gotschalk, C., Ladd, T. M., Siegel, D. A., Welch, Z. S., Iglesias-Rodriguez, M. *et al.* 2019. Formation, development, and propagation of a rare coastal coccolithophore bloom. *Journal of Geophysical Research: Oceans*, 124: 3298–3316.
- Mehrbach, C., Culbertson, C. H., Hawley, J. E., and Pytkowicz, R. M. 1973. Measurement of the apparent dissociation constants of carbonic acid in seawater at atmospheric pressure. *Limnology and Oceanography*, 18: 897–907.

- Meyer, J., and Riebesell, U. 2015. Reviews and Syntheses: responses of coccolithophores to ocean acidification: a meta-analysis. *Biogeosciences*, 12: 1671–1682.
- Müller, M., Antia, A., and LaRoche, J. 2008. Influence of cell cycle phase on calcification in the coccolithophore *Emiliana huxleyi*. *Limnology and Oceanography*, 53: 506–512.
- Müller, M., Trull, T. M., and Hallegraeff, G. M. 2017. Independence of nutrient limitation and carbon dioxide impacts on the Southern Ocean coccolithophore *Emiliana huxleyi*. *The ISME Journal*, 11: 1777–1787.
- Omar, A. M., Olsen, A., Johannessen, T., Hoppema, M., Thomas, H., and Borges, A. V. 2010. Spatiotemporal variations of $f\text{CO}_2$ in the North Sea. *Ocean Science*, 6: 77–89.
- Raven, J. A., and Beardall, J. 2005. Respiration in aquatic photolithotrophs. *In Respiration in Aquatic Ecosystems*, pp. 36–46. Ed. By P. A. del Giorgio and P. J. L. B. Williams Oxford University Press, New York. 315 pp.
- Raven, J. A., Gobler, C. J., and Hansen, P. J. 2020. Dynamic CO_2 and pH levels in coastal, estuarine, and inland waters: theoretical and observed effects on harmful algal blooms. *Harmful Algae*, 91: 101594.
- Ritchie, R. J. 2006. Consistent sets of spectrophotometric chlorophyll equations for acetone, methanol and ethanol solvents. *Photosynthesis Research*, 89: 27–41.
- Rokitta, S., and Rost, B. 2012. Effects of CO_2 and their modulation by light in the life-cycle stages of the coccolithophore *Emiliana huxleyi*. *Limnology and Oceanography*, 57: 607–618.
- Sabine, C. L., Feely, R. A., Gruber, N., Key, R. M., Lee, K., Bullister, J. L., Wanninkhof, R. *et al.* 2004. The oceanic sink for anthropogenic CO_2 . *Science*, 305: 367–371.
- Schaum, C. E., Rost, B., and Collins, S. 2016. Environmental stability affects phenotypic evolution in a globally distributed marine picoplankton. *The ISME Journal*, 10: 75–84.
- Schlüter, L., Lohbeck, K. T., Gröger, J. P., Riebesell, U., and Reusch, T. B. H. 2016. Long-term dynamics of adaptive evolution in a globally important phytoplankton species to ocean acidification. *Science Advances*, 2: e1501660.
- Smith, H. E. K., Tyrrel, T., Charalampopoulou, A., Dumousseaud, C., Legge, O. J., Birchenough, S., Pettit, L. R. *et al.* 2012. Predominance of heavily calcified coccolithophores at low CaCO_3 saturation during winter in the Bay of Biscay. *Proceedings of the National Academy of Sciences of the United States of America*, 109: 8845–8849.
- Strickland, J. D. H., and Parsons, T. R. 1972. A practical handbook of seawater analysis. Fisheries Research Board of Canada Bulletin, 167: 49–80.
- Suffrian, K., Schulz, K. G., Gutowska, M. A., Riebesell, U., and Bleich, M. 2011. Cellular pH measurements in *Emiliana huxleyi* reveal pronounced membrane proton permeability. *New Phytologist*, 190: 595–608.
- Sunda, W. G., Price, N. M., and Morel, F. M. 2005. Trace metal ion buffers and their use in culture studies. *Algal Culturing Techniques*, 4: 35–63.
- Vargas, C. A., Lagos, N. A., Lardies, M. A., Duarte, C., Manriquez, P. H., Aguilera, V. M., Broitman, B. *et al.* 2017. Species-specific responses to ocean acidification should account for local adaptation and adaptive plasticity. *Nature Ecology and Evolution*, 1: 0084.
- White, M. M., Drapeau, D. T., Lubelczyk, L. C., Abel, V. C., Bowler, B. C., and Balch, W. M. 2018. Calcification of an estuarine coccolithophore increases with ocean acidification when subjected to diurnally fluctuating carbonate chemistry. *Marine Ecology Progress Series*, 601: 59–76.
- Wolf-Gladrow, D., and Riebesell, U. 1997. Diffusion and reactions in the vicinity of plankton: a refined model for inorganic carbon transport. *Marine Chemistry*, 59: 17–34.
- Xu, J., Bach, L. T., Schulz, K. G., Zhao, W., Gao, K., and Riebesell, U. 2016. The role of coccoliths in protecting *Emiliana huxleyi* against stressful light and UV radiation. *Biogeosciences*, 13: 4637–4643.
- Xu, K., Gao, K., and Hutchins, D. A. 2020. Measurements of calcification and silicification. *In Research Methods of Environmental Physiology in Aquatic Sciences*, pp. 269–276. Springer, Singapore.
- Zhang, Y., Bach, L. T., Lohbeck, K. T., Schulz, K. G., Listmann, L., Klapper, R., and Riebesell, U. 2018. Population-specific responses in physiological rates of *Emiliana huxleyi* to a broad CO_2 range. *Biogeosciences*, 15: 3691–3701.
- Zhang, Y., Collins, S., and Gao, K. 2020. Reduced growth with increased quotas of particulate organic and inorganic carbon in the coccolithophore *Emiliana huxleyi* under future ocean climate change conditions. *Biogeosciences*, 17: 6357–6375.

Handling editor: Shubha Sathyendranath